Civil Engineering Infrastructures Journal 2022, 55(2): 223-240
DOI: 10.22059/CEIJ.2021.315974.1731

RESEARCH PAPER

# Numerical Study of the Failure in Elbow Components of Buried Pipelines under Fault Movement

**Salimi Firoozabad, E.[1], Samadzad, M.[2] and Rafiee-Dehkharghani, R.[2*]**

[1] Ph.D., School of Civil Engineering, College of Engineering, University of Tehran, Tehran, Iran.
[2] Assistant Professor, School of Civil Engineering, College of Engineering, University of Tehran, Tehran, Iran.

© University of Tehran 2021

Received: 25 Dec. 2020; Revised: 16 Jul. 2021; Accepted: 02 Aug. 2021

**ABSTRACT:** Faults have large impact on the mechanical behavior of soil in pipeline's construction. These pipelines have been embedded to supply vital resources such as water, oil, and gas for consumers. To prevent damage, it is highly recommended not to construct pipelines around active faults. However, it is generally inevitable to cross the fault due to wide extension of pipelines. In this paper, a numerical analysis and parametric study on an underground water pipeline in Tehran, Iran, under the fault-induced displacement is presented. It is important to note that the main focus of this study is on elbow components which are the most critical sections in pipeline systems. The effects of crossing angle, distance to elbow and various soil properties on the elbow response are investigated. It is aimed at finding a safe regulation to embed pipelines with the lowest level of risk expected in elbow components after fault movement. The results show that the elbow component does not suffer serious damage when the crossing angle is 90°, provided they are not located in the close vicinity of the fault rupture surface. However, when the crossing angle decreases to 60 and 45 degrees, these components are much more vulnerable.

**Keywords**: Buried Pipelines, Elbow, Failure, Fault Movement, Soil-Pipe Interaction.

## 1. Introduction

Buried pipelines are considered as lifelines that human's life highly depends on them. These lifelines carry water, oil, and gas throughout residential areas in major cities for consumers. They are mostly steel made and manufactured in different pieces (for convenient transportation) including straight parts, elbows, and tee sections to be assembled and welded in sites. Steel pipe elbows are one of the most common sections used in pipelines to convey fluids. Pipelines are often exposed to existing fault movement as they are expanded all around under the ground passing through the fault lines. Therefore, they could be damaged or even failed to supply consumers. It is observed that the elbow components are one of the most critical parts in pipeline systems that are very vulnerable to fault rupture.

Elbow components have been reported to be the most critical points of different pipelines and piping systems including

* Corresponding author E-mail: rezarafiee@ut.ac.ir

nuclear power plants (Salimi Firoozabad et al., 2015), subsea pipelines (Pouraria et al., 2017) and buried pipelines (Vazouras and Karamanos, 2017). The failure analysis of various types of steel pipe elbow due to the cyclic loading by Salimi Firoozabad et al. (2016), and low-cycle fatigue (Varelis and Karamanos, 2015; Hassan et al., 2015) has been studied in the literature. Extensive experimental studies on the structural behavior of steel elbows (Varelis et al., 2013; Hassan et al., 2015; Kiran et al., 2018; Kim et al., 2019) have been also performed.

There are numerous studies in the literature on analysis of buried pipelines crossing active faults. Newmark and Hall (1975) developed a method for analyzing the effect of a fault movement on a pipeline. They found that the pipeline capacity in buried soil depends mainly on the fault movement, soil characteristics, fault angle, slip length, and pipe material specifications. Karamitros et al. (2011), proposed an analytical methodology for the strain analysis of elbows subjected to permanent ground deformation. More recently, Tsatis et al. (2019) studied failure modes of buried pipeline and effective parameters crossing normal and reverse faults. Sabermahani and Bastami (2019) considered rotation between the cross-section and the bending line due to the shear deformations for the stress analysis of a buried pipeline. These few available FEA studies on pipe elbows in the literature are either analytical or scaled, they propose an application process, surrounding soil modeling, and loading condition, quite difficult (time consuming) to be applied on a real pipeline case. Furthermore, Majrouhi Sardroud et al. (2021) indicated the importance of having BIM adopted for urban piping systems to evaluate the risk of rupture in case of an earthquake.

The pipe-soil interaction was studied by Kokavessis and Anagnostidis (2006). they used the finite element method and contact elements to describe the soil-pipe interaction and analyzed buried pipes under permanent motion of the earth. More recently, Vazouras, et al. (2015, 2017) studied the mechanical behavior of buried straight pipes and also pipe bends crossing different fault angles by using the Finite Element Method (FEM), considering different failure criteria. Bildik and Laman (2015) performed experiments on buried pipes in sand box subjected to a vertical static load in order to conduct a parametric study on soil's bearing capacity. In addition, Castiglia et al. (2018) studied the performance of buried pipelines in liquefied soil considering the effect of pore water pressure and structure's floatation.

Elbow components have been reported to be one of the most critical points of different pipelines and piping systems although, their behavior under fault movement has not been much investigated. Therefore, the structural behavior of pipe elbow components in a real buried pipeline crossing fault line has been studied in this paper. Various parameters have taken into considerations including soil mechanical properties, soil-pipe interaction properties, fault angle, and distance to elbow. Full scale three dimensional existing pipelines and surrounding soil are modeled. A real water transmission pipeline geometry (used in Tehran metropolitan city, Iran) is taken as a case study for numerical simulation. The reliability of the simulations has been verified by two different experiments: 1) A centrifuge test on a buried polyethylene pipeline under fault movement; and 2) A test on a steel pipe elbow under monotonic and cyclic loading.

## 2. Finite Element (FE) Modeling

The structural response of the steel pipe under fault movement is studied using numerical calculations. For this purpose, the general finite element method (FEM) program ABAQUS/Implicit (2016) is used for simulating the mechanical behavior of the steel pipeline, the surrounding soil environment, and their interaction in a precise manner, considering the detailed geometry of the soil and pipe along their

nonlinear material properties.

### 2.1. Pipeline Description

A small part of real water transition pipeline (used in district 4 of Tehran metropolitan city, Iran) is taken as a case study for numerical simulation as shown in Figure 1. The pipeline has a total length of 197.75 meters (m), including two straight parts 63, 133 m, and an elbow, with curvature radius to diameter ratio of $r/D = 2.5$, connecting those two parts (Figure 2). The pipeline diameter ($D$) and thickness (t) are 0.5 m and 5.2 mm, respectively, which has the diameter to thickness ratio of $D/t = 96$. The pipeline's material is Carbon Steel ASTM (ASTM, 2011) SA-53 GR-A with the material properties (given by Salimi Firoozabad et al., 2015): ρ = mass density = 7850 kg/m$^3$, E = Young's Modulus = 203509 MPa, ν = Poisson's Ratio = 0.3. It is assumed that the material has plastic behavior with Kinematic Hardening rule, and first yielding occurs at 310 MPa. The pipeline is meshed using an 8-node linear brick solid element (element C3D8R from ABAQUS element library). Using a mesh convergence analysis, the minimum mesh size is selected to be equal to 0.0625 m in cross section. However, the mesh size increased linearly to 0.125 m in farther regions from the elbow to alleviate the computational burden.

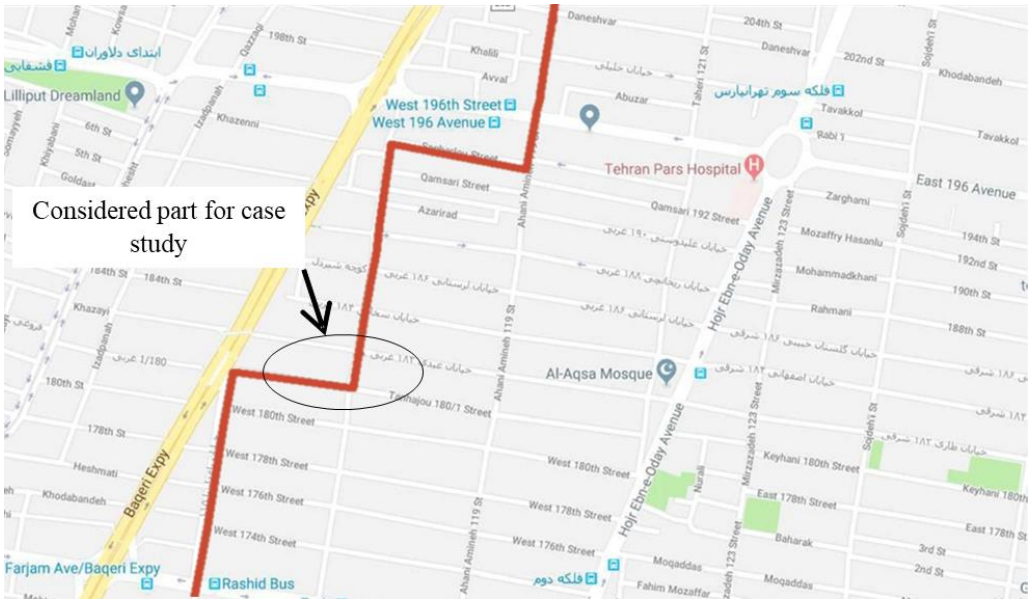


**Fig. 1.** Tehran's pipeline map and the section considered in this research

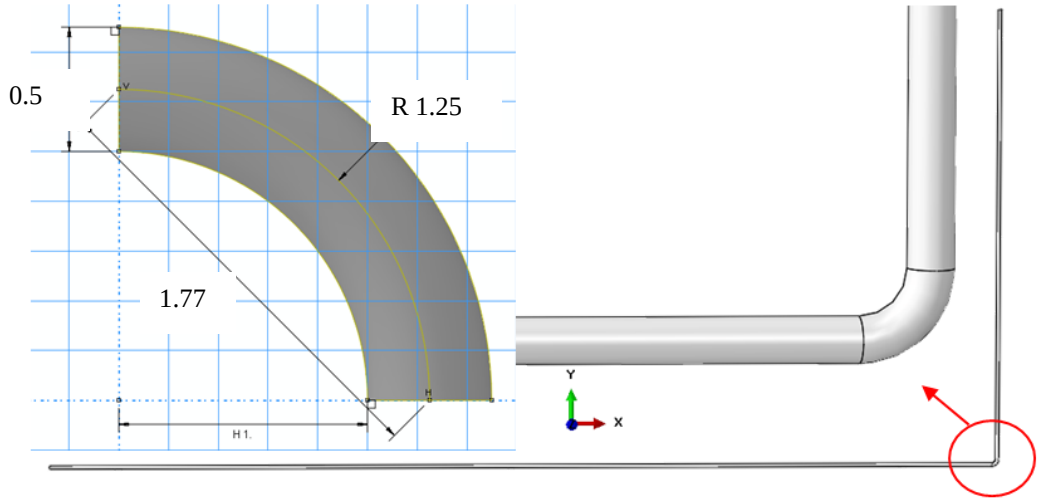


**Fig. 2.** The pipeline and the elbow geometry (numbers unit is m)

## 2.2. Soil Characteristics

The soil material properties are selected considering the geotechnical reports about different locations in Tehran, Iran. Within this context, the density, elastic modulus, and Poisson's ratio parameters are considered to be 2000 kg/m$^3$, 50.5 MPa, and 0.35, respectively. The soil is modeled as a block with a rectangular cross section having the width and height of 6 and 2.5 m, respectively, which allows the pipe's burial depth to be equal to 2D as suggested in Vazouras et al. (2015). It should be noted that the ground should be first excavated for embedding the pipe and filled later to cover it. This causes the change in material properties of the soil above the pipe. To consider this issue, the filled soil is modeled with the new properties as: $\rho$ = 1600 kg/m$^3$, E = 30 MPa and $\nu$ = 0.35. This is shown schematically in Figure 3. The soil plastic behavior is based on Mohr-Coulomb plasticity criteria which have been reported to be well matched to real soil characteristics in the literature by Anastasopoulos et al. (2007) and Loukidis et al. (2009). Considering the geotechnical data, the friction angle ($\varphi$) and cohesion is selected to be 34° and 15 kPa (Motallebiyan et al., 2020), respectively. The dilation angle ($\psi$) is considered to be zero. The soil is modeled using 8-node linear brick solid C3D8R elements with a mesh size range of 0.25 (in cross section) to 0.5 m (along the model).

The procedure to draw the surrounding soil proposed in the literature (Vazouras et al., 2015) is that the soil is drawn as a complete rectangular box. However, the soil in this study is taken with a constant geometry along the pipeline's length in order to significantly reduce the number of soil elements. It should be noted that the soil section size is taken based on the recommendations available in the literature and also the sensitivity analysis performed to ensure that the boundaries do not affect the results. For example, the pipe's burial depth is selected to be equal to 2D as suggested in Vazouras et al. (2015). Furthermore, the obtained results also confirm that such soil size is sufficient as stress contour tend to be negligible at the soil surface.

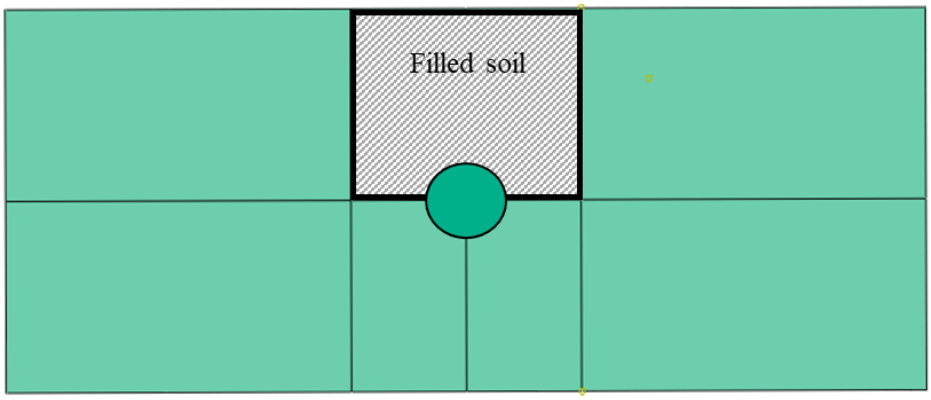


**(a)**

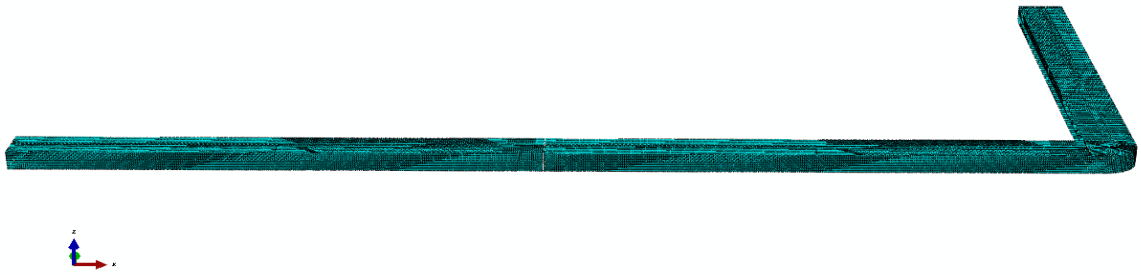

**(b)**

**Fig. 3.** Soil domain in FE analyses: a) Cross section; and b) Geometry

### 2.3. Loading and Boundary Conditions

Faults are fractures in the earth crust, with rocks on both sides moving against each other. Each fault (inclined) can be considered a surface, which divides rocks on its both sides into two parts. Tehran is surrounded and cut by several major faults (shown with redlines in Figure 4 according to Ritz et al., 2012). Therefore, it is very probable that any buried lifeline system would certainly cross one of those faults. Faults, based on the nature of their movement, are categorized into four types as strike-slip, normal, reverse, and oblique. It is generally stated (Hessami and Jamali, 2006) that the existing faults in Iran are mostly fall into strike-slip types, cause damages on the elbow crossing over them due to the axial deformation. Hence, a strike-slip fault is considered in this paper for investigating its effect on the pipeline passing through it. In this case, the soil is divided into two parts (exactly in the middle of the longer straight part) including the fixed part and the movable part. Therefore, the fault movement is applied horizontally (Y axis) on the vertical surface (Y-Z surface) of the movable part (see Figure 5). The movement was applied statically as the fault moves slowly in real cases and it is assumed to be equal to one meter (in total). It must be noted that the location of the fault and its crossing angle is subjected to change in the simulations in order to investigate the influence of these parameters on the behavior of elbow.

Generally, the FE analysis is divided into major three steps. First the geostatic step is run to establish the interaction between soil and pipe and calculating the geostatic stresses. The second step relates to applying the internal pressure of the pipe which is equal to 2 MPa according to the design pressure for these pipelines (ASME Boiler and Pressure Vessel Code II Part D, 2007). Finally, in the third step, the fault movement is applied as a displacement loading with the total value of 1 m in 10 seconds (with maximum increments set at 0.1 m). Note that the effect of nonlinear geometry is also accounted in the modeling.

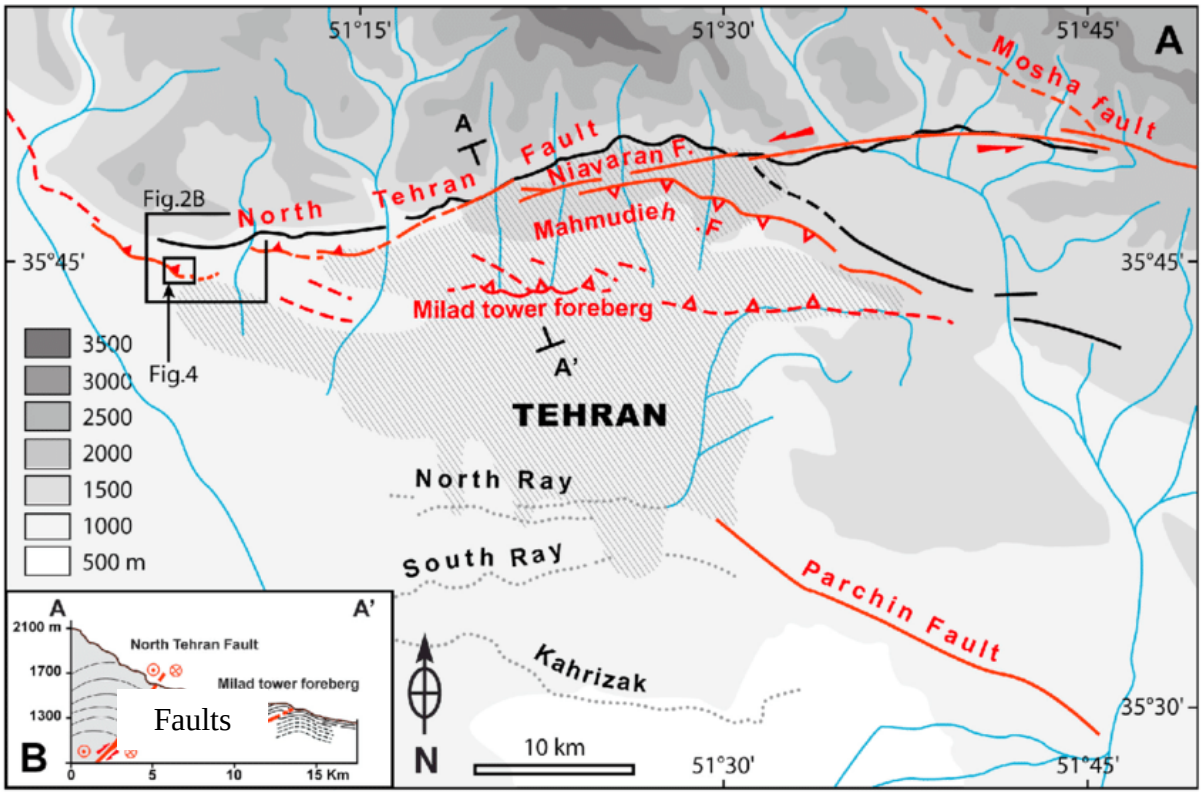


**Fig. 4.** Tehran's fault lines map (Ritz et al., 2012), (the red lines are the major fault lines)

Different types of boundary conditions are carefully applied to various parts of the model in order to represent the physics behind the model. Within this context, the boundary of the soil domain is fixed in all simulation steps. In addition, the horizontal movement of vertical surfaces of the soil was also constrained at the first two steps and set to be free in only movable part in the last step when the fault movement was applied. The pipeline was also horizontally constrained at both ends in the first two steps (since it is assumed that it is connected to the rest of the pipeline) while it is set as free at the end of the moving part at the last step.

One of the most important parameters in the analysis of buried pipelines is the interaction between the soil and pipe. It is mostly due to this parameter that fault movement affects the pipelines, which can lead to minor and major damages in these lifelines. A surface to surface interaction between soil and pipe material has been defined for this purpose, and a penalty based friction formulation has been adopted for the tangential behavior of the interaction with the friction coefficient set to 0.44 ($\tan(0.7\,\varphi)$) by Dash and Jain (2007).

## 3. FE Model Verification

In order to ensure the reliability of the FE simulation steps, which requires proper selection of material properties, soil-pipe interaction characteristics, and load/boundary conditions, it is required to compare and validate the results with a series of related analytical, laboratory or field works. For this purpose, a qualitative comparison is presented between the results of an experiment conducted in RPI, USA by Ha et al. (2008) on a polyethylene buried pipe subjected to normal fault and the FE numerical model generated in this research. In addition, the numerical results related to the behavior of a steel pipe elbow component under static load is verified with that of an experiment performed in South Korea by Salimi Firoozabad et al. (2016).

### 3.1. Verification for a Buried Pipe

In order to ensure the validity of numerical simulations, its results should be compared to those of the experiments. As it was not possible to conduct a test in this study, the reported experiments available in literature are used for verification. Consequently, the results of the tests conducted in RPI, USA on polyethylene pipes and surrounding soil subjected to a normal fault were extracted and compared with the simulations' results in this paper. The numerical simulations are performed using commercial ABAQUS FE software (2016). The details of the simulations are selected according to the specifications and characteristics presented in Ha et al. (2008) study. The experiment setup and soil surface deformation are shown in Figure 6. The specification of the pipe and the soil and the characteristics of its materials are as follows:

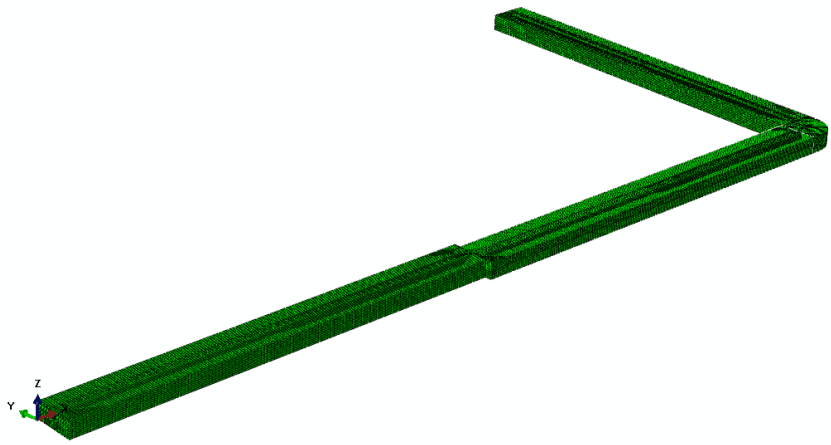


**Fig. 5.** The deformed FE model after applying the fault movement

High Density Polyethylene (HDPE) pipe for water service (AWWA Standard C901, 2003) with the diameter of 33.4 mm, thickness of 1.96 mm, and length of 1.14 m. The material properties are given in Table 1. The soil around the pipe was modeled as a solid cube, with the length, width, and thickness of 1.14 m, 0.76 m, and 0.2 m, respectively. The soil domain is divided (from the mid-point) into two fixed and moving parts. The soil domain was then assigned a material with the properties as given in Table 1.

The fault is normal and a 40 mm displacement was applied downward and perpendicular to the soil surface. To simulate the fault movement, a displacement loading is applied at the bottom of the soil in the movable part while the bottom of the fixed part was restrained in all directions. The simulation results, after applying the fault movement, are shown in Figure 7. Considering the element sizes of the soil and pipe in Figure 7, and significance of the mesh size in interaction analysis, it should be noted that a robust verification is made through the experiments, and it is observed that the mesh size needs to be selected carefully to capture the structural behavior of the soil and the pipe accurately. As for the soil-pipe interaction, the mesh size of soil is the same through the connected surface with the pipe and double the size through the pipe length. The same size was used in simulation verification with the experiment conducted in RPI, USA by Ha et al. (2008).

**Table 1.** The material properties of the performed experiment in Ha et al. (2008)

| Material | Density ($kg/m^3$) | Elastic modulus (MPa) | Poisson's ratio | Friction angle (degree) | Cohesion coefficient (kPa) |
|---|---|---|---|---|---|
| HDPE Pipe | 958 | 880 | 0.4 | N/A | N/A |
| Soil | 1498 | 42.747 | 0.35 | 0 | 15 |

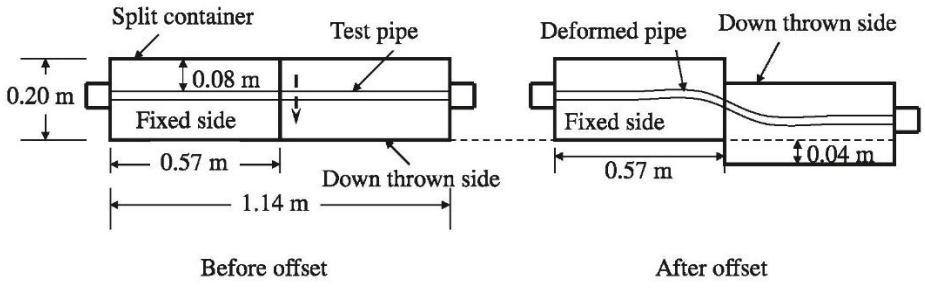


**(a)**

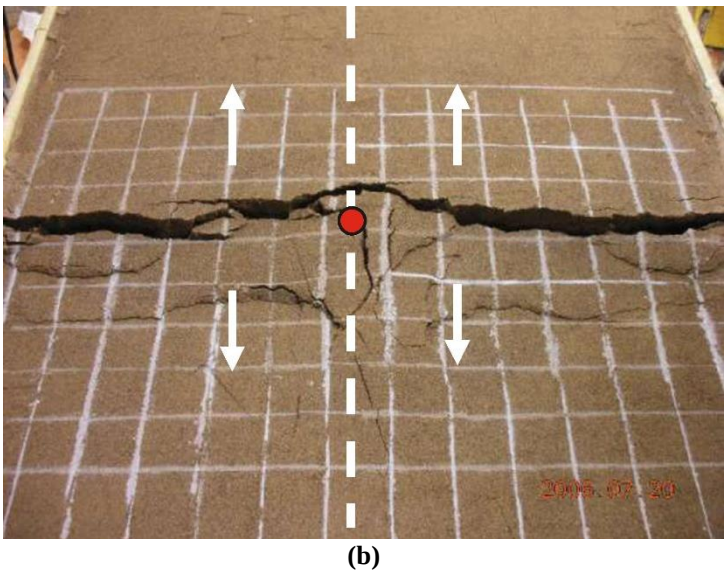

**(b)**

**Fig. 6.** a) Experiment setup; and b) Soil surface deformation at the end of experiment (Ha et al., 2008)

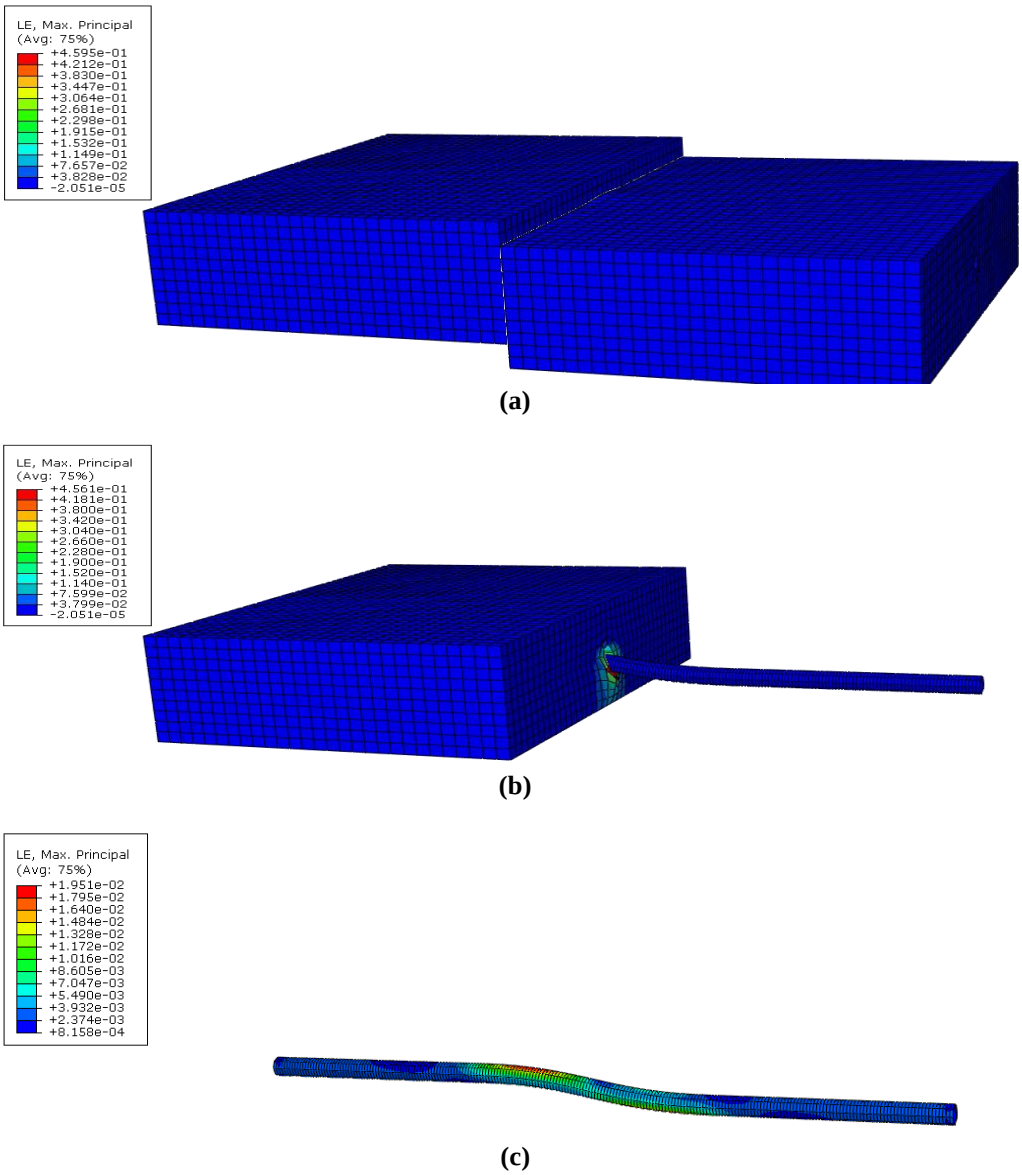


**Fig. 7.** Maximum principal stain after application of fault movement: a) Soil; b) Soil and pipe; and c) Pipe

The axial and flexural strain across the pipe were compared with that of the experiment as shown in Figure 8. Note that the experiment was carried out under the gravity acceleration of 12.2g, and the same gravity value is employed in the numerical simulation. Due to this reason, the axial and flexural strains extracted along the pipe at different locations, the distance between these points, and the distance from the fault location, are multiplied by the scaling factor of 12.2.

According to the results in Figure 8 and considering the uncertainties associated with the difference between the real material properties, loading and boundary conditions, and other modeling details, it can be concluded that there is a good agreement between the experimental and numerical simulations, which proves the fidelity of the FE simulations. One of the major reasons of the existing difference between the results can be attributed to the plastic behavior of polyethylene pipes. This type of behavior is modeled using a simple kinematic plastic behavior due to the lack of information for using more complex material properties. Besides, in our simulations, a steel pipeline was used which is separately verified and discussed subsequently. Hence, it could be reasonably implied that the FE simulation was reliable enough to be used in the presented case study.

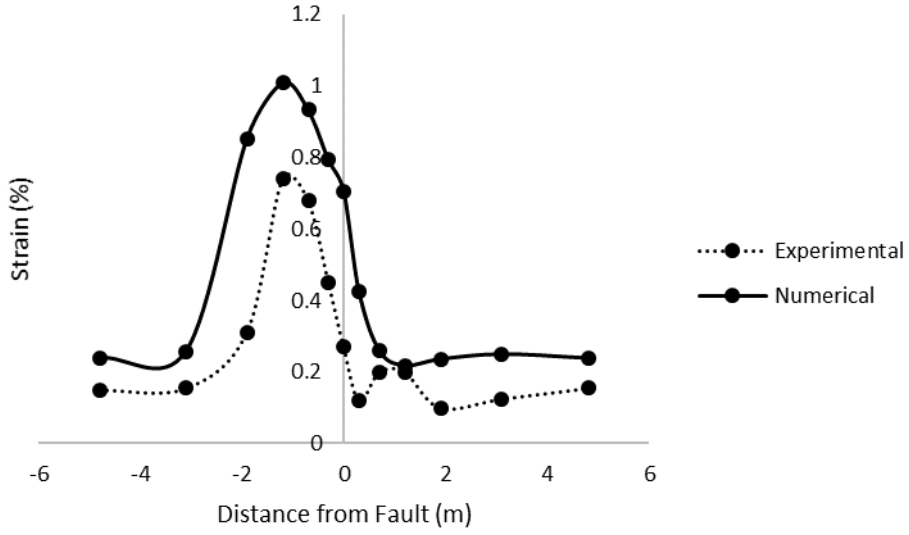


**(a) Comparison of axial strain**

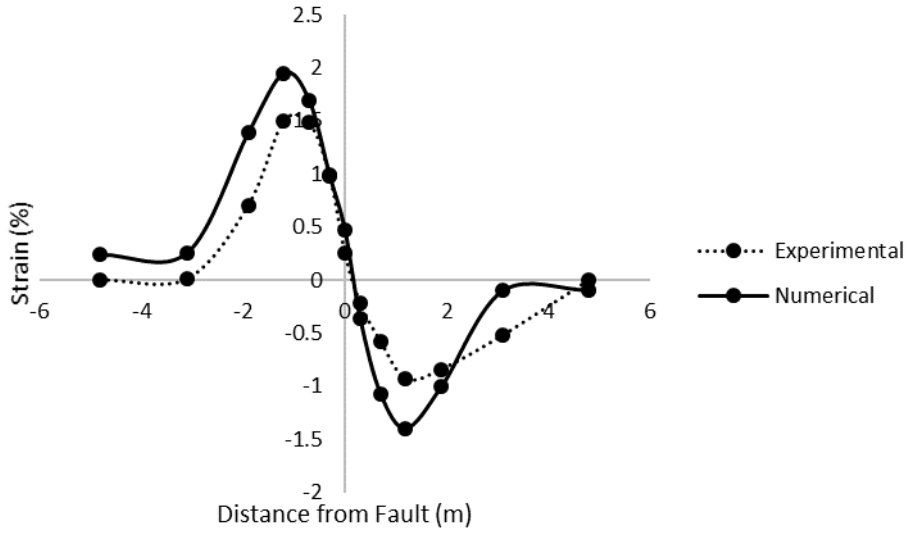


**(b) Comparison of bending strain**

**Fig. 8.** The axial and flexural strain comparison between experimental and numerical analysis

### 3.2. Verification of Steel Pipe Elbow Simulation

The pipeline simulation has been verified by comparing it with a series of experiments performed on actual test specimens. The experiments were performed by the first author (of this paper) in the Department of Civil Engineering at Pusan University, Pusan, South Korea. The specimen was a 0.075 m (3 inches) elbow component (Figure 9) with similar characteristics as our case study pipeline (Carbon Steel ASTM SA-53 GR-A) with the density of $\rho = 7850$ kg/m$^3$, elastic modulus of $E = 203509$ MPa, and a Poisson's ratio of $\nu = 0.3$. The test setup and detailed descriptions are provided in Salimi Firoozabad et al. (2016). The component was first subjected to an internal pressure of 3 MPa and thereafter a series of various monotonic and cyclic displacement loadings are applied. The elbow is fixed in all directions except the rotation along its axis. The other end of the elbow is the location where it is subjected to gradual displacement loading with the maximum speed of 36 mm/min.

The mechanical properties of the elbow, its geometry, boundary conditions, and loading are simulated in accordance with the experiments performed. Kinematic hardening rule is used in order to simulate

the plastic behavior of the component, as this rule is more accurate as the elbow is loaded cyclically both in tension and compression. In the numerical analysis, an internal pressure is first applied in a static step then, a cyclic displacement equal to 60 mm is applied as the next step. Similar to the pipeline, the elbow is modeled using C3D8R solid elements from ABAQUS element library. It should be noted that shell elements can also be used for modeling the pipeline. However, it is found that for contact (interaction) simulation between soil and pipe, solid elements provide more accurate results and are computationally more efficient. Furthermore, solid elements are used for modeling the elbow and they are tied to the beam elements as shown in Figure 9. The mesh size is selected to be 5 mm even though it converged at 10 mm. The difference is not that much but for dynamic analysis, 5 mm would be the better choice. It is worthwhile to mention that tying the end nodes of solid elements to the beam constrains all displacements of the nodes of the exposed faces of the solid elements to remain to the cross-sectional plane. The cross-sectional plane is in turn characterized by six degrees of freedom and constrained to the six degrees of freedom on the end node of the beam element. This is performed in order to be able to handle boundary conditions at the fixtures which are connected to the ends of the elbowed pipe.

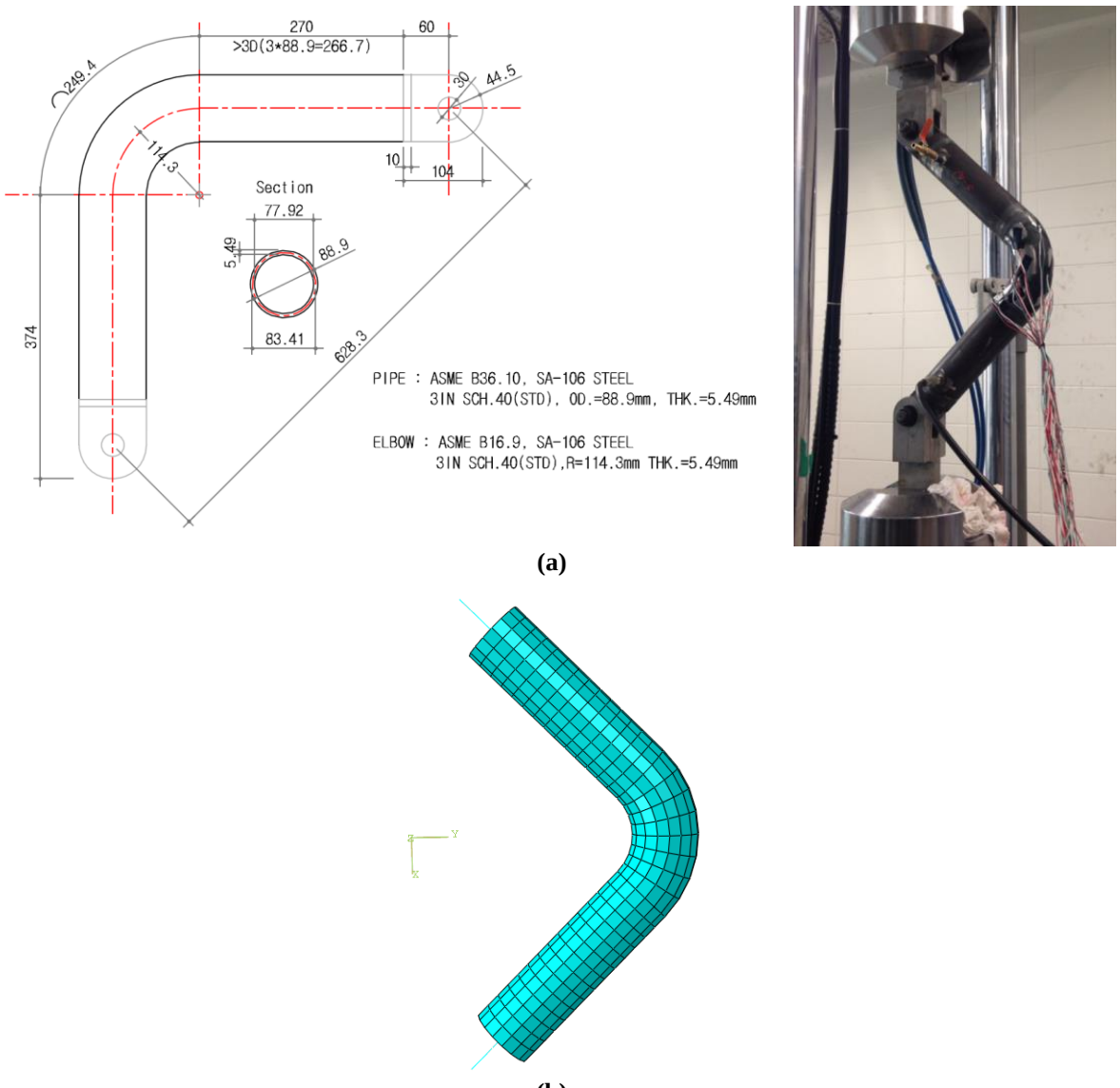


**Fig. 9.** a) The elbow specimen in Salimi Firoozabad (2016); and b) FE numerical model

The result of numerical static analysis is compared with the experiments using ± 60 mm cyclic displacement in the X direction to one end of the elbows while the other end is fixed. The results are shown in Figure 10 as the force-displacement graph at the point of applied displacement, in the experiment and simulation. It can be seen that the difference between numerical result and the actual sample is negligible. This proves the reliability of the used kinematic hardening model, and therefore, it is used for FE modeling of the buried pipeline in this paper.

## 4. Failure/Yield Criterion

The exact structural failure point of a steel pipe elbow has not yet been fully estimated. Therefore, various criteria have been defined, expressed and examined in the literature and standard code provisions. These criteria are mostly expressed for straight pipes based on a limit state defined in tension and compression. Consequently, tensile and compressive stress and/or strain capacities are evaluated. A cross sectional distortion limit is also defined in some cases due to local buckling. It must be noted that fault movement causes large plastic strains; therefore, pipeline performance is better to be evaluated in terms of longitudinal strain, rather than stress. This means that the fault movement is clearly governed by a displacement-controlled based scenario.

The tensile strain capacity of the steel pipe is highly dependent on the fracture of pipe wall and it is controlled by the strength of pipe at the welding point, so that the stress and strain rate at the weakest point in the pipe results in defective welding. This capacity has been considered in a range of approximately 2 to 5 percent in the literature as explained in the following references. Canadian Standard Association (CSA Z662) (2007) proposes an empirical equation based on parameters including: weld toughness, the yield-tensile strength ratio, and defect height and length ratio over the pipe wall thickness. This value would lay in a range of 3 to 5 percent based on general values. EN1998-4 provisions (1998) and ASCEMOP119 (2009) also suggest 3% in the case of buried steel pipelines subjected to fault movement. ASME code provision for Boiler and Pressure Vessel (2007) adopts a so-called Twice Elastic Slope (TES) method for strain limit calculations. Furthermore, a value of 1 to 2 percent is recommended for normal operation of hydrocarbon pipelines by Pipeline Research Council International (2004).

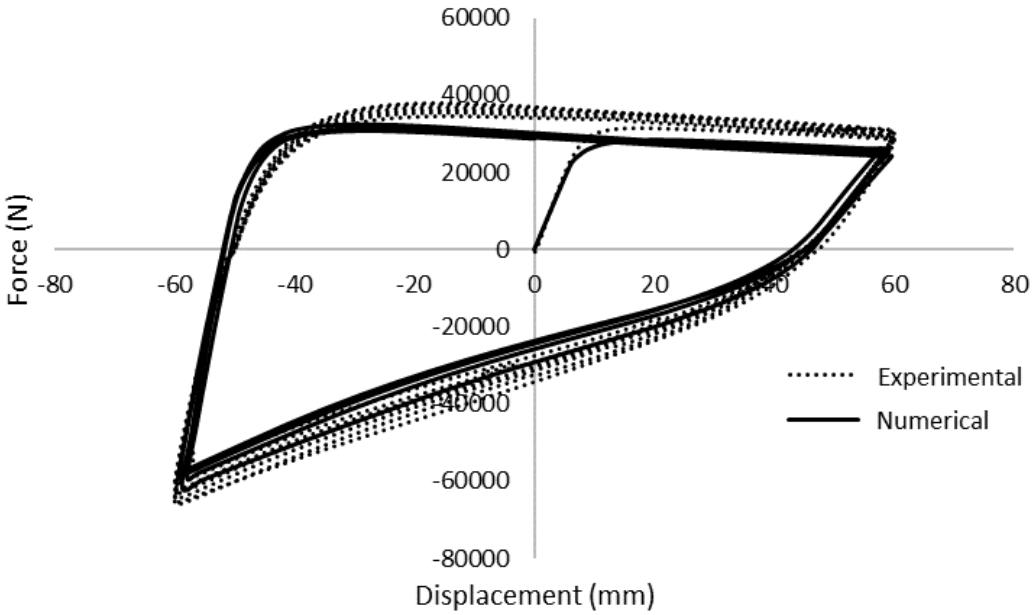


**Fig. 10.** Comparison of experimental and numerical results in force-displacement graph

Due to the vital importance of elbow components, the capacity limit in this study is considered to be the lowest of the above-mentioned values. For this purpose, it is required to calculate the capacity of the elbow based on TES method. Hence, a numerical simulation has been performed on a steel pipe elbow with the exact same geometry and material properties, as the pipeline elbow in this research. An internal pressure equal to 2 MPa is firstly applied and then a gradually increasing static load is applied to one end as an incremental increasing displacement. Accordingly, the elbow is free to move at one end and fixed on the other. Figure 11 shows the geometry, loading, and boundary conditions (BCs) of the simulated elbow and stress contour after load application.

As it can be seen in Figure 11, the location of the critical point is in the internal part of the curvature at the middle of the elbow. The same location is identified as maximum stress critical point in the numerical simulation of buried pipeline, which verifies the correct application of load and BCs. Accordingly, the force and strain of that point is extracted, and the corresponding graph is derived and shown in Figure 12. The line in which the slope is twice the elastic line's slope is drawn. Hence, the intersection of this line and the stress-strain curve would indicate the strain limit which in this case is 0.009 (shown in Figure 12). Given that this amount is less than the other indicated values for tensile limit state, 0.009 is selected as the final capacity in this study and the results of the failure analysis of the pipeline crossing over the fault is compared with this value.

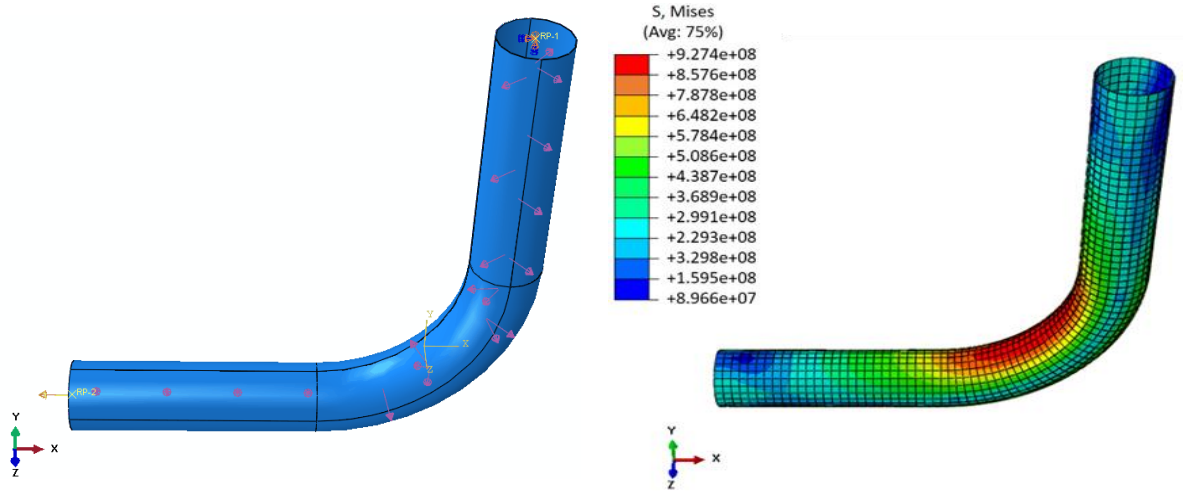


**Fig. 11.** a) Geometry; and b) Von Mises stress contour results of the elbow

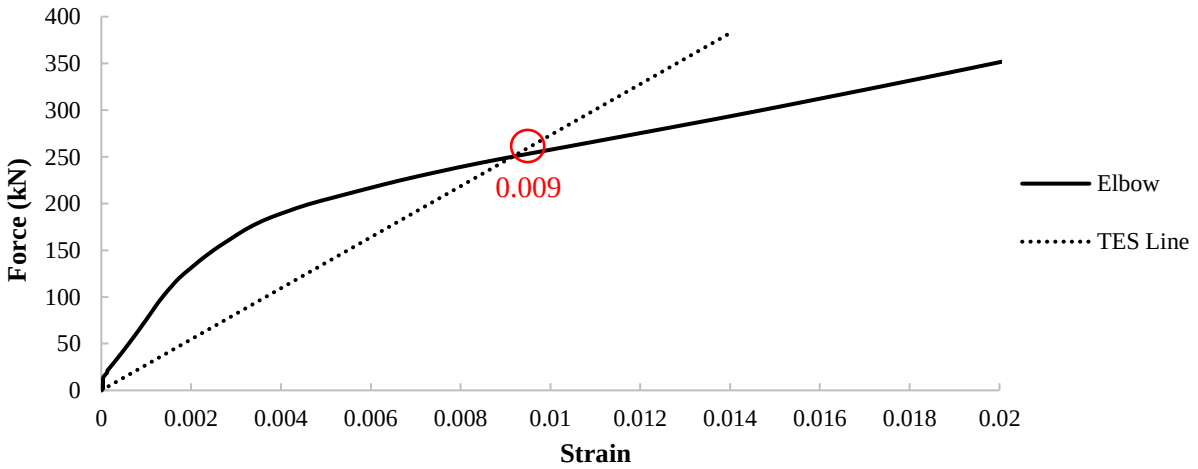


**Fig. 12.** Force-strain graph at the critical point of the elbow

## 5. Results and Discussion

### 5.1. Effect of Angle and Distance to Elbow

In this section, the results of numerical simulation of the pipeline under displacements induced by a strike-slip fault are presented. The effect of two important parameters on the behavior of elbow joint in the pipeline has been investigated. These two parameters are: the angle of fault crossing the pipeline and the elbow joint distance from the fault location. For this purpose, three fault line angles of 90, 60, and 45 degrees are considered with respect to the axis of the pipeline. In addition, three values for the distance of the fault location to the elbow is considered: 68 m (middle of the soil length), 53 m, and 38 m from the elbow. Therefore, a total of 9 simulations (given in Table 2) have been performed. The distances are not taken further closer to the elbow as the study is more focused on the strain in elbow caused by the soil-pipe interaction rather than the results caused by bending due to the fault movement itself. The affected range of pipeline in length crossing over a fault proposed by Karamitros et al. (2011) is 35 to 45 times of pipe diameter (17.5 to 22.5 m in this study) on both sides of the fault. Hence, the minimum distance of fault to elbow is taken 38 m which is outside of the range to be influenced by fault movement.

The structural behavior of the elbow is then expressed as its maximum principal strain response for each simulation case. Then, the results are compared with the failure criterion in order to identify the most critical case. This critical case is next taken for evaluation of the effect of soil properties on the elbow component response. Finally, some practical recommendations are presented for engineering practice.

The fault movement is uniformly applied perpendicular to the horizontal surface of the soil in the moving part. It should be noted that the maximum displacement of 100 cm is considered for fault movement and it is gradually applied in 1000 increments.

In the FE simulations where the fault line is perpendicular to the soil, the elbow did not show any displacement due to the fault movement. It happened in all cases even when the fault is in the nearest considered distance to elbow (38 m). It is observed that the pipeline suffers no damage approximately 10 m from the fault line on each side. Consequently, the elbow would be safe unless it is well close to the fault line. In addition, the maximum Von Mises stress (480 MPa) and strain (0.02) observed is around the fault line on both sides as it is expected. Figure 13 shows the maximum Von-Mises stress of the pipeline after the fault movement is applied in the simulation case in which the fault line is occurred at the distance of 38 m from the elbow.

In the next three cases, the fault movement is applied to the soil with crossing angle of 60°, and three different distances from the elbow. The maximum strain within the elbow in the first two cases is insignificant. However, in the last case (Figure 14), where the fault distance to elbow is 38 m, it reaches to 0.0045.

**Table 2.** Simulation cases

| Simulation No. | Simulation name | Fault crossing angle | Distance to elbow |
|---|---|---|---|
| 1 | A1 | 90 | 68 |
| 2 | A2 | 90 | 53 |
| 3 | A3 | 90 | 38 |
| 4 | B1 | 60 | 68 |
| 5 | B2 | 60 | 53 |
| 6 | B3 | 60 | 38 |
| 7 | C1 | 45 | 68 |
| 8 | C2 | 45 | 53 |
| 9 | C3 | 45 | 38 |

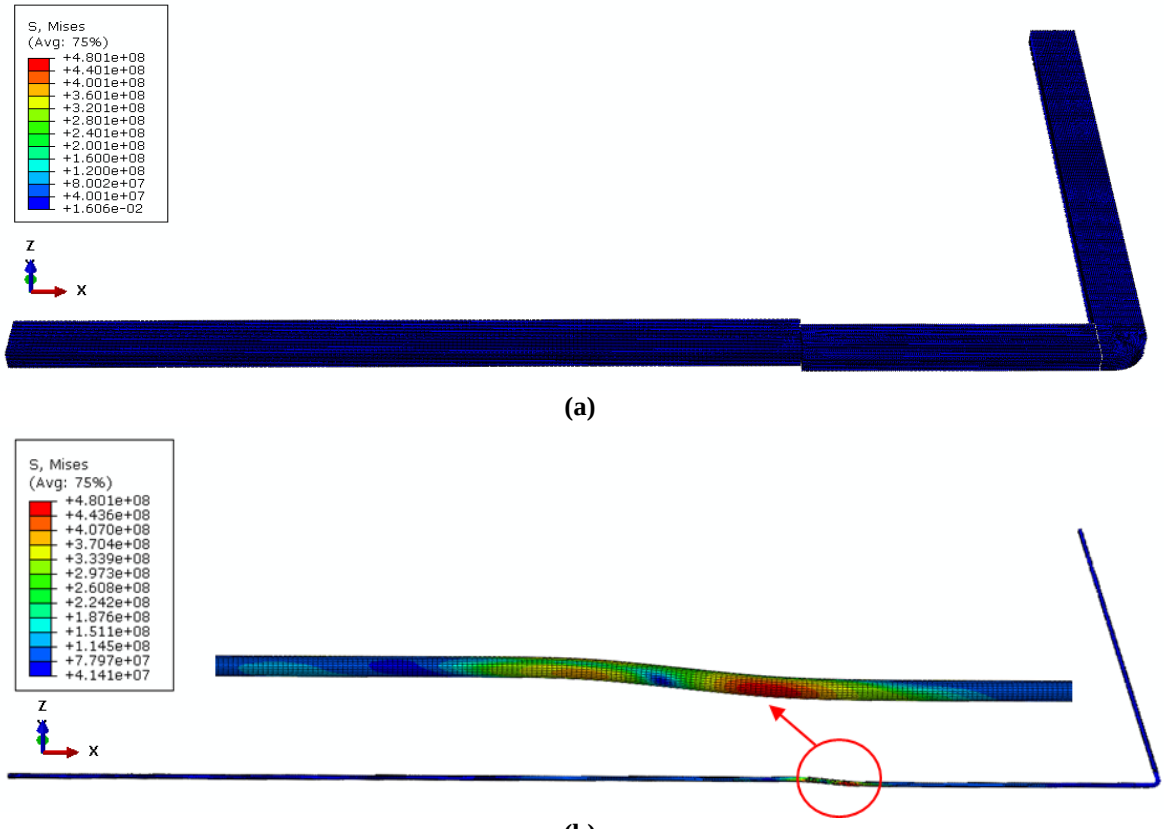


**Fig. 13.** The Von Mises stress contour in: a) Soil; and b) Pipeline (simulation A3)

Finally, three more simulations with the fault distance to elbow of 68, 53, and 38 m are performed for crossing angle of 45°. It is observed that the elbow undergoes no strain in the first case, then the strain reaches to 0.001 in the second case, and it reaches to the peak of 0.01 when the distance to elbow is 38 m. Hence, the elbow suffers a significant damage beyond the failure criterion when the fault crosses the pipeline at 38 m from the elbow with 45°. Figure 15 shows the stress contour for pipeline subjected to fault movement in the last simulation case, along the logarithmic strain contour in elbow. It can be seen that the most critical point of the elbow is exactly the same point as the one identified in failure criterion estimation of the elbow (given in Section 3).

Different simulations and analysis scenarios indicate that when the pipeline passes through the fault perpendicularly, the deformations and strains in the pipeline vanishes at short distances from the fault (about 7.5 m), so the rest of the pipeline would be safe. The reason could be attributed to the effect of soil continuity on both sides of the fault and the pipe flexibility along its length. On the other hand, when the pipeline crosses the fault with an angle less than 90°, the fault movement has both vertical and horizontal components. The horizontal component, considering the volume of soil and its interaction with the pipe, loads the pipe in the axial direction, which causes significant increase in the strain rate of the elbow.

### 5.2. Effect of Soil Properties

It is observed in the previous section that the most critical simulation case is when the crossing angle is 45° and it is located at the distance of 38 meter from the elbow. Therefore, this case is selected for the parametric study on the effect of soil properties on the elbow performance. The varying soil properties considered for the parametric study are: elastic modulus, cohesion, and friction angle. All these parameters considered as two different values (within the range for sandy clay type of soil based on Unified Soil Classification

System (USGS) (2011)) other than the original values. The elastic modulus is taken as 35 and 70 MPa, the cohesion is selected to be 30 and 45 kPa, and the friction angles are set to be 30 and 40 degrees. It must be noted that the friction coefficient, for the interaction between soil and pipe, changes accordingly for each friction angle value. Hence, another six simulations are performed and their corresponding principal strains are extracted and compared.

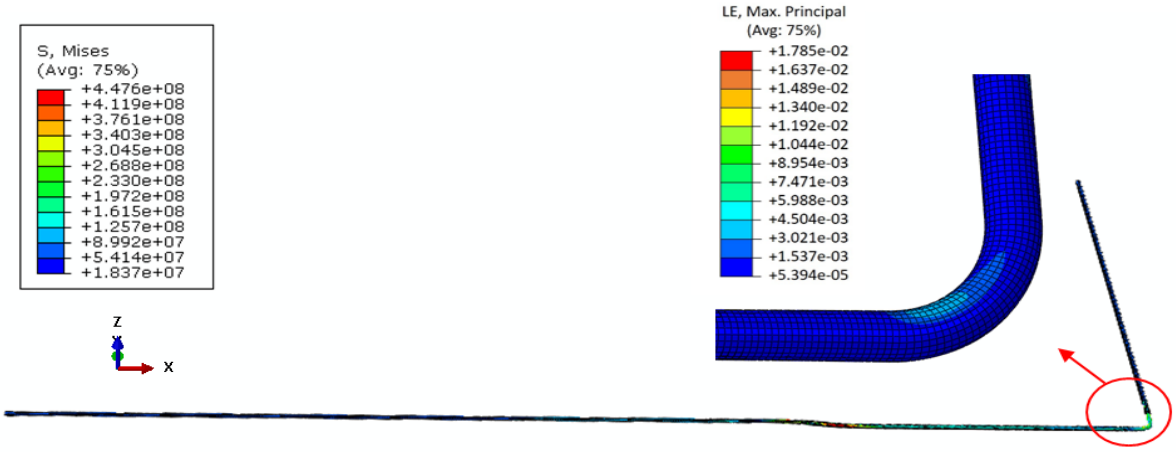


**Fig. 14.** The stress and strain contour in pipeline and elbow (Simulation B3)

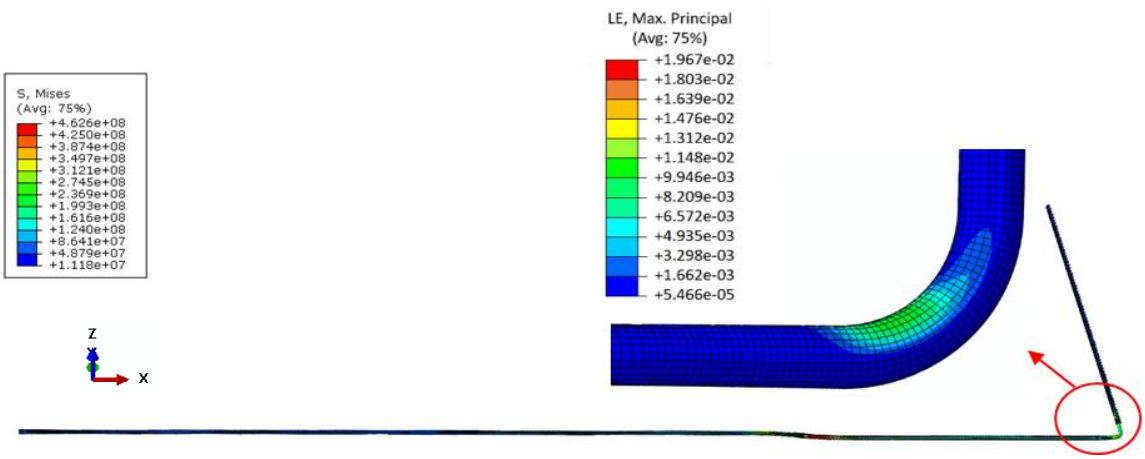


**Fig. 15.** The stress and strain contour in pipeline and elbow (Simulation C3)

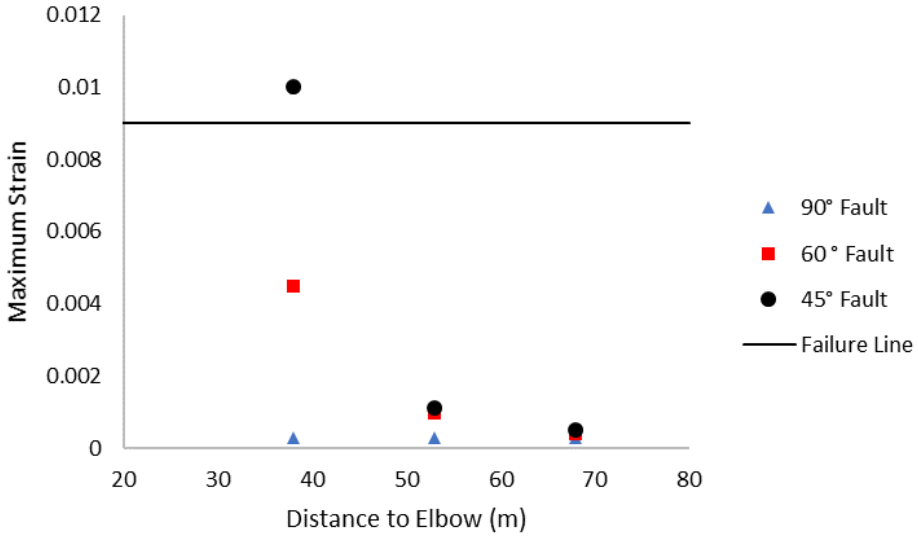


**Fig. 16.** Results of all simulations

It is observed that the cohesion changes would not significantly affect the elbow performance. Then, the elastic modulus which is originally 50.5 MPa, changed to 35 and 70 MPa. In this case also, an increase in elastic modulus did not make a significant change in final results. The friction angle on the other hand, has a considerable impact on the elbow, approximately 85 percent in ten degrees. The strain value is 0.007 at friction angle 30°, 0.013 at 40° friction angle. Therefore, the higher value of friction angle leads to higher strain level as it is expected because it changes the friction coefficient which increases the applied displacement at elbow due to fault movement.

It is noted that the strain variation in straight part of pipeline around the fault in different cases are more significant. Figure 17 shows the strain versus distance from fault results for all six simulation cases for different soil properties. Strain variation can be seen for each soil properties and it can be compared with the original soil properties.

Most standard provisions highly recommend not constructing around any active fault due to the severity of the damage as a result of fault movement. However, in the case of pipelines construction, it is inevitable to cross the fault due to the large length of these pipelines. One of the most common sections used in pipelines are steel pipe elbows. These sections must be analyzed and checked with an extra care as they are more vulnerable (due to less failure capacity) than straight sections in pipelines. However, their behavior under fault movement has not been much investigated. Therefore, there are not much of any recommendations on their safety evaluation crossing over active faults. Accordingly, available recommendations for straight pipes in the literature have been expanded on the elbow sections.

The numerical analysis and parametric study conducted on a real case of water transmission pipelines indicated the importance of elbow failure analysis. For instance, it is understood that the elbow could be damaged at the farther distance to a fault as much as 38 m (68D, i.e. 68 times of pipe diameters), which is quite significant. Other researchers such as Karamitros et al. (2011) have reported smaller ranges of 35 to 45D on either side of the crossing fault. It is observed when the pipeline crosses over a fault, the safe distance to fault line for elbow to be placed, is highly dependent on crossing angle. Another effective parameter in elbow safe performance is the internal angle of friction of soil. On the contrast, the soil's cohesion, and elastic modulus has a negligible effect on the pipeline behavior.

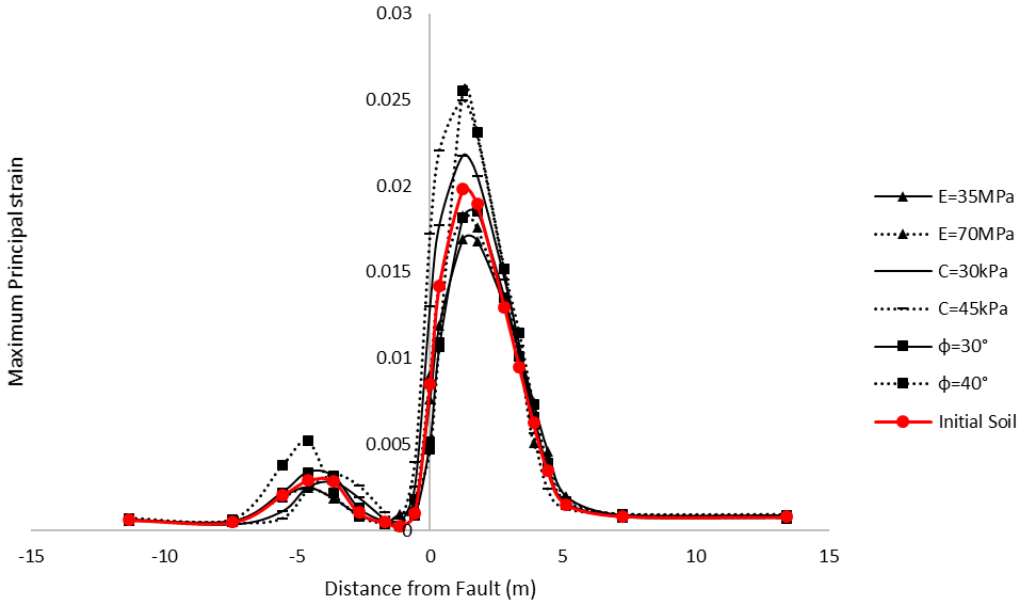


**Fig. 17.** Strain variation around the fault line for all soil properties

## 6. Conclusions

A numerical analysis was performed on a buried water transmission pipeline. The simulations were verified with the experimental data reported in the literature. The elbow component's behavior was investigated through a defined failure criterion. The effects of fault crossing angle and distance to elbow was also investigated. Furthermore, the soil characteristics effects on the elbow's response was evaluated.

Different simulations and analysis scenarios indicated that: when the pipeline crosses perpendicular to a strike-slip fault, the deformations and strains in the pipeline vanishes at short distances from the fault (about 7.5 m) so an elbow would be safe in a distance more than 7.5 m. On the other hand, when the pipeline crosses the fault with an angle less than 90°, the fault movement had both vertical and horizontal component. The horizontal component applied displacement loading on the pipe in the horizontal direction, which caused the strain rate to increase in the elbow. A safe distance for the elbow from the fault was then estimated as 38 and 53 m for the crossing angle of 60 and 45°, respectively.

It was observed that the soil cohesion changes would not significantly affect the elbow performance. In the case of elastic modulus also, the variations did not make a significant change in the final results. The friction angle on the other hand, had a considerable impact on the elbow, approximately 85 percent in ten degrees. The strain value was 0.007 at friction angle 30°, 0.013 at 40° friction angle.

## 7. Recommendation for Future Study

A more comprehensive study including more numerical analysis considering other crossing angles, pipe and elbow geometry and soil properties can lead to comprehensive recommendation and safety regulations for underground pipelines design.

## 8. References


ABAQUS/Standard. (2016) *User's manual*, Providence, RI, USA: Simulia.

American Society of Mechanical Engineers (ASME). (2007). *Boiler and pressure vessel code*, NY, United States.

American Water Works Association. (2003). *AWWA standard for polyethylene (PE) pressure pipe and tubing, 1/2 in. (13 mm) through 3 in. (76 mm), for water service*, ANSI/AWWA C901-02, Denver, Colorado, United States.

Anastasopoulos, I., Gazetas, G., Bransby, M.F., Davies, M.C.R. and El Nahas, A. (2007). "Fault rupture propagation through sand: finite-element analysis and validation through centrifuge experiments", *Journal of Geotechnical and Geoenvironmental Engineering*, 133(8), 943-958.

ASTM Committee D-18 on Soil and Rock. (2011). *Standard practice for classification of soils for engineering purposes (Unified Soil Classification System)*, ASTM International, West Conshohocken, PA, USA.

Bildik, S. and Laman, M. (2015). "Experimental investigation of the effects of pipe location on the bearing capacity", *Geomechanics and Engineering*, 8(2), 221-235.

Canadian Standard Association. (2007). *Oil and gas pipeline system*, Z662–07, Ottawa, ON, Canada.

Castiglia, M., Santucci de Magistris, F. and Napolitano, A. (2018). "Stability of pipelines in liquefied soils: Overview of computational methods", *Geomechanics and Engineering*, 14(4), 355-366.

Dash, S.R. and Jain, S.K. (2007). *Guidelines for Seismic Design of buried pipelines*, IITK-GSDMA Codes, National Information Center of Earthquake Engineering, Indian Institute of Technology, Kanpur, India.

De Normalisation, Comité Européen. (1998). *Eurocode 8, Part 4: Silos, tanks and pipelines*, CEN EN 4, European Committee for Standardization, Brussels, Belgum.

Firoozabad, E.S., Jeon, B.G., Choi, H.S. and Kim, N.S. (2015). "Seismic fragility analysis of seismically isolated nuclear power plants piping system", *Nuclear Engineering and Design*, 284, 264-279.

Firoozabad, E.S., Jeon, B.G., Choi, H.S. and Kim, N.S. (2016). "Failure criterion for steel pipe elbows under cyclic loading", *Engineering Failure Analysis*, 66, 515-525.

Ha, D., Abdoun, T.H., O'Rourke, M.J., Symans, M.D., O'Rourke, T.D., Palmer, M.C. and Stewart, H.E. (2008). "Buried high-density polyethylene pipelines subjected to normal and strike-slip faulting, A centrifuge investigation", *Canadian Geotechnical Journal*, 45(12), 1733-1742.

Hassan, T., Rahman, M. and Bari, S. (2015). "Low-cycle fatigue and ratcheting responses of elbow piping components", *Journal of Pressure Vessel Technology*, 137(3), 031010-1 to 12.

Hessami, K. and Jamali, F. (2006). "Explanatory notes to the map of major active faults of Iran", *Journal of Seismology and Earthquake Engineering*, 8(1), 1-11.

Honegger, D.G. and Nyman, D.J. (2004). *Guidelines for the seismic design and assessment of natural gas and liquid hydrocarbon pipelines*, Pipeline Research Council International, Inc., Arlington, Va. Catalogue, (L51927).

Karamitros, D.K., Bouckovalas, G.D., Kouretzis, G.P. and Gkesouli, V. (2011). "An analytical method for strength verification of buried steel pipelines at normal fault crossings", *Soil Dynamics and Earthquake Engineering*, 31(11), 1452-1464.

Kim, S.W., Jeon, B.G., Hahm, D.G. and Kim, M.K. (2019). "Seismic fragility evaluation of the base-isolated nuclear power plant piping system using the failure criterion based on stress-strain", *Nuclear Engineering and Technology*, 51(2), 561-572.

Kiran, A.R., Reddy, G.R. and Agrawal, M.K. (2018). "Experimental and numerical studies of inelastic behavior of thin walled elbow and tee joint under seismic load", *Thin-Walled Structures*, 127, 700-709.

Kokavessis, N.K. and Anagnostidis, G. (2006). "Finite element modelling of buried pipelines subjected to seismic loads: Soil structure interaction using contact elements", In: *Proceedings of the ASME PVP conference*, Vancouver, BC, Canada.

Loukidis, D., Bouckovalas, G.D. and Papadimitriou, A.G. (2009). "Analysis of fault rupture propagation through uniform soil cover", *Soil Dynamics and Earthquake Engineering*, 29(11-12), 1389-1404.

Majrouhi Sardroud, J., Fakhimi, A., Mazroi, A., Ghoreishi, S.R., Azhar, S. (2021). "Building information modeling deployment in oil, gas and petrochemical industry: An adoption roadmap", *Civil Engineering Infrastructures Journal*, 54(2), 281-299.

Motallebiyan, A., Bayat, M. and Nadi, B. (2020). "Analyzing the effects of soil-structure interactions on the static response of onshore wind turbine foundations using Finite Element method", *Civil Engineering Infrastructures Journal*, 53(1), 189-205.

Newmark, N.M. and Hall, W.J. (1975). "Pipeline design to resist large fault displacement", In: *Proceedings of US National Conference on Earthquake Engineering*, pp. 416-425.

Pouraria, H., Seo, J.K. and Paik, J.K. (2017). "Numerical study of erosion in critical components of subsea pipeline: Tees vs bends", *Ships and Offshore Structures*, 12(2), 233-243.

Ritz, J.F., Nazari, H., Balescu, S., Lamothe, M., Salamati, R., Ghassemi, A., Shafei, A., Ghorashi, M. and Saidi, A. (2012). "Paleoearthquakes of the past 30,000 years along the North Tehran Fault (Iran)", *Journal of Geophysical Research: Solid Earth*, 117(B6).

Sabermahany, H. and Bastami, M. (2019). "Refinement to the existing analytical methods of analysis of buried pipelines due to strike-slip faulting", *Civil Engineering Infrastructures Journal*, 52(2), 309-322.

Tsatsis, A., Loli, M. and Gazetas, G. (2019). "Pipeline in dense sand subjected to tectonic deformation from normal or reverse faulting", *Soil Dynamics and Earthquake Engineering*, 127, 105780.

Varelis, G.E., Karamanos, S.A. and Gresnigt, A.M. (2013). "Pipe elbows under strong cyclic loading", *Journal of Pressure Vessel Technology*, 135(1), 011207.

Varelis, G.E. and Karamanos, S.A. (2015). "Low-cycle fatigue of pressurized steel elbows under in-plane bending", *Journal of Pressure Vessel Technology*, 137(1), 011401-1 to 10.

Vazouras, P. and Karamanos, S.A. (2017). "Structural behavior of buried pipe bends and their effect on pipeline response in fault crossing areas", *Bulletin of Earthquake Engineering*, 15(11), 4999-5024.

Vazouras, P., Dakoulas, P. and Karamanos, S.A. (2015). "Pipe–soil interaction and pipeline performance under strike, Slip fault movements", *Soil Dynamics and Earthquake Engineering*, 72, 48-65.

This article is an open-access article distributed under the terms and conditions of the Creative Commons Attribution (CC-BY) license.